Estimating Blood Flow Velocity in Liver Vessels

Michael Müller[1], René Keimling[1], Sascha Lang[1], Josef Pauli[1], Uta Dahmen[2], Olaf Dirsch[2]

[1]Informatik und Angewandte Kognitionswissenschaft, Uni Duisburg-Essen
[2]Klinik für Allgemein-, Viszeral- und Transplantationschirurgie, Uniklinikum Essen
michael_mueller@uni-due.de

Abstract. Orthogonal polarization spectroscopy (OPS) is a technique for taking images to finally characterise microcirculation. Current image analysis algorithms have limitations when applied to image sequences obtained from the liver. We developed an automatic analysis tool which enables detection of liver vessels, measurement of vessel diameters, and determination of blood flow velocities with sparse user interactions. For validation purpose, data was analysed with our proposed algorithm and compared with manual results by experienced users. Related to commercial products, the needed time for analysis is reduced from more than 30 minutes to less than 2 minutes with comparable results for accuracy.

1 Introduction

This article covers the problem field of automatic characterisation of blood flow through the liver, i.e. liver perfusion, which is important for the assessment of regeneration after parial liver resection [1]. Orthogonal Polarization Spectroscopy (OPS) is a non-extensive technology, avoiding radiation, enabling high spatial and temporal resolution. It is useful for noninvasive in vivo measurements of hepatic microcirculation in small liver vessels (sinusoids) of the same individual repeatedly [2]. OPS-based commercial products like CapiScope [3] or MicroScan [4] need continual time-consuming user interactions, e.g. for vessel detection. Recently, an academic OPS-based system for the analysis of sublingual or cardiac microcirculation has been published [5], but no experiments were reported for liver perfusion which would have to cope with higher densities of vessels and lower signal-to-noise ratios. We aimed at developing an OPS-based tool allowing an automated analysis of liver perfusion with a minimum of user interactions.

2 Materials and methods

We first describe the sensing device for taking image sequences, then describe the methods for sinusoid detection, including image preprocessing, foreground/background separation, and skeletonisation, and finally describe the methods relevant for velocity measurement in a sinusoid, including also width analysis of sinusoids and the placing of virtual sensors in sinusoid sections.

OPS visually records the blood flow in microscopical scale within the liver tissue at $0.5mm$ beneath the surface. Polarised green light is sent towards the target tissue and the reflections are perceived by a CCD camera. At the surface a part of the light is reflected, within the tissue the remaining light is dispersed by most of the cells and absorbed by the red blood-cells (erythrocytes). Using an additional orthogonally oriented polarisation filter, the light from the surface is suppressed and only the light dispersed from the tissue interior will reach the camera. A lens is used for magnification leading to a spatial resolution of approximately 450 pixel/millimeter. The flow of erythrocytes appear as moving dark blobs and surrounding tissue as bright. Typically, image sequences of 375 images are taken in a period of 15 seconds with a refreshing rate of 50 fields/second. Problems with image processing originate from low signal-to-noise ratio, unbalanced illumination, and motion blur. The latter is due to unavoidable, external movement of the hand-held camera as well as respiratory and cardiac actions of the animal. In our work, image sequences from the liver tissue of rats are analysed in the context of experimental surgery.

Four steps treat the problems with illumination and noise (Fig. 1a). Histogram equalisation is applied to each image individually in order to increase the contrast. Then, the mean gray levels of all images are measured, the global mean brightness is computed, and the mean gray levels of all images are adjusted to that global mean. Next, noise is removed from each image using a median filter, that does not affect image structures too much. Finally, different gray levels in various image parts, caused by unbalanced illumination, are nomalised using a maximum filter for shading correction.

The set of sinusoids is defined as foreground and the remaining tissue as background. Apart from clearly visible sinusoids there are additional sinusoids which are hardly detectable in a single image. But the motion of erythrocytes encodes additional information concerning presence of sinusoids. This finding is included in the binarisation process which consists of five steps. a) All images of the sequence are combined into one aggregated image using a special median filter that operates on corresponding pixels in the temporal context (rather than spatial). b) The resultant aggregate image is binarised using local histograms for adaptive thresholding. c) Artefacts at the image border, caused by the limited aperture, are removed by image clipping to a circular shape. d) Salt-

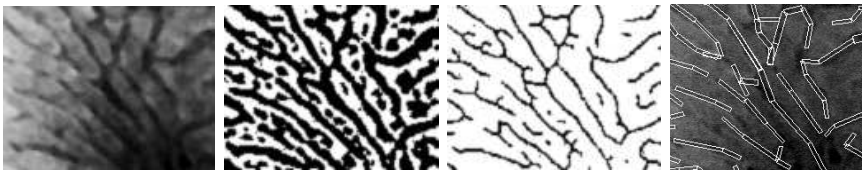

(a) (b) (c) (d)

Fig. 1. (a) Original image with unbalanced illumination. (b) Binarised image of sinusoids and some artefacts. (c) Removal of artefacts and skeletonisation. (d) Rectangular sinusoid areas for placing virtual sensors.

and-pepper noise is removed by morphological opening and closing operations: e) Non-sinusoid regions are detected and removed, using morphological hit-or-miss operations which consider the region shapes and the local background. The remaining regions are candidate areas for sinusoids (Fig. 1b).

A further hit-or-miss operation is applied repeatedly for a skeletonisation of this candidate regions, leading to curved center lines. Occasionally, this basic procedure will remove important parts of the network of lines, which in turn have to be recovered again. The line end points are detected and Gestalt laws like smooth continuation and neighborhood are applied. Further methods are responsible for treating splitting, converging, or crossing lines (Fig. 1c).

By counting the number of iterations during skeletonisation, also the width of the sinusoid regions can be obtained. For the subsequent method of analysing velocities, so-called virtual sensors are placed into sinusoid sections. A virtual sensor is a small area (e.g. square) of pixels from which the gray levels are recorded. Two such sensors are treated as pair and placed at a certain offset in the sinusoid. Rectangular areas are embedded into sinusoid sections, wherein to place the sensor pairs and thereby making sure that both sensors are nearby and from the same sinusoid. From the skeleton curves, straight line segments of maximal lengths are constructed respectively, whose end points lie on the curve and whose intermediate points lie completely within the width of the considered part of the sinusoid region. These straight line segments are used in combination with the stored diameters to create the rectangular areas (Fig. 1d).

The flow of erythrocytes in sinusoids is observable as movement of dark blobs surrounded by slightly brighter pixels. However, the gray values of the pixels in the image sequence are exposed to intense noise. An explicit blob extraction would be unreliable and time-consuming and is therefore avoided. Instead, the gray values of a virtual sensor area are combined to a scalar value using an adequate filter (e.g. median or Gaussian), and recorded in the course of time, leading to a one-dimensional signal. From a pair of sensors in a sinusoid section we obtain two similar, time-shifted signals. Based on normalised cross-correlation of the two signals we compute the time-shift more reliably. It is obtained as maximum correlation value for a certain time-shift value. Auto-correlation is used for normalisation.

For increasing the reliability of velocity measurement the following strategy is applied: a) Based on prior experiments the optimal sensor configuration is chosen in the rectangular area of a sinusoid. b) A cross-correlation value related to a sensor pair is only accepted if a certain threshold is exceeded. c) The percentage of accepted cross-correlation values must exceed a further threshold, and these set of values are fused alternatively by two types of algorithms, i.e. computing the mean or the median (MeanCCA or MedCCA).

3 Results

The automatic detection has been validated with measures of precision ($\frac{TP}{TP+FP}$) and recall ($\frac{TP}{TP+FN}$), which consider true positives (TP), false positives (FP),

Sequ.	TP	FP	FN	Precision	Recall
1	10500	2800	3100	78,95%	77,21%
2	11200	1200	2800	90,32%	80,00%
3	10500	1700	3600	86,07%	74,47%
4	10500	2600	3300	80,15%	76,09%
5			mean value	83,87%	76,94%
6			standard deviation	9,19%	4,03%

Table 1. Results for sinusoid detection, including precision and recall values for four image sequences, mean values and standard deviations.

and false negatives (FN). TP is the number of pixels of the skeleton curves of sinuisoids both extracted automatically and manually, FP is the number of pixels extracted only automatically, FN is the number of pixels extracted only manually. Fig. 2 shows exemplary an overlay of automatic and manual sinusoid detection (green for TP, red for FP, blue for FN). The precision value should exceed a certain threshold, otherwise too many measurements are taken in non-sinusoid areas. Also the recall value must exceed a certain threshold, otherwise too many sinusoids are not considered for velocity measurements. In average, precision and recall is about 84 % and 77 % with a standard deviation of 9% and 4%, respectively (Tab. 1).

Considering a sinusoid, the ground truth of velocity of blood flow has to be compared with the results of automatic estimation. However, the ground truth is initially unknown and will be estimated manually. For this purpose a graphical user interface is used to place a dynamic black-white pattern in the image near to a real sinusoid and then to adjust the velocity of the movable black squares to finally be synchronous with the velocity in the sinusoid (Fig. 3). For the automatic estimation several measurements from different pairs of sensors are combined by computing the mean or median cross-correlation. For velocity estimation, several image sequences were treated, several sinusoids were considered therein, the manual estimations of the experienced users were logged, and the algorithm with median cross-correlation was applied (Tab. 2). Ground truth estimation is done by 10 users leading to a coefficient of variation 0.22. For the results produced by the algorithm this coefficient is 0.37.

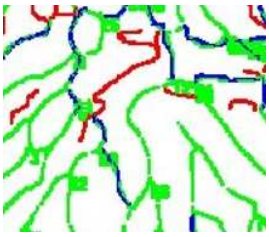

Fig. 2. Overlay of automatic and manual sinusoid detection.

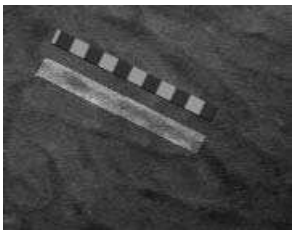

Fig. 3. Sinusoid section, dynamic pattern to estimate velocity ground truth.

Table 2. Typical velocity estimations for four image sequences by an experienced user and by the two types of the algorithm.

Sequ.	Manually [mm/sec]	MeanCCA [mm/sec]	MedCCA [mm/sec]
1	0.60	0.60	0.50
2	0.65	0.75	0.70
3	0.30	0.35	0.25
4	0.40	0.45	0.40

4 Discussion

The algorithm automatically detects sinusoids, selects the relevant and reliable ones, and estimates the blood flow velocity therein. For the purpose of reproducibility we refer to the theses of Keimling and Lang [6] for details like binarisation thresholds, morphological structure elements, correlation thresholds, and other parameters. Evaluations have shown acceptable precision and recall values (84% and 77%) for sinusoid detection. Concerning velocity estimations, manual and automatic responses are similar, but the coefficient of variance is still larger for the algorithm (0.37 versus 0.22). Due to the automatisation of sinusoid detection and selection, the liver perfusion can be characterised in less than 2 minutes, as opposed to more than 30 minutes by formerly used systems [3, 4]. Currently, we conduct more systematic experiments and evaluations in order to find out the degree of acceptability by relevant medical experts. Future work may be devoted to a further improvement of the accuracy of velocity estimations, and to the automatic selection of unblurred sections in image sequences.

References

1. Fogli L, Gorini P, Cappellari L, et al. Effect of partial hepatectomy and liver regeneration on portal pressure in rats. Surgical Research Comm. 1990;6:159–166.
2. Puhl G, Schaser K, Vollmar B, et al. Noninvasive in vivo analysis of the human hepatic microcirculation using OPS imaging. Transplantation. 2003;75:756–761.
3. KKTechnology. Cam1 and CapiScope User Manual. Honiton, Devon, England; 2004. http://www.kktechnology.com/help/book1.html, visited 02.01.2009.
4. MicroVisionMedical. MicroScan. Amsterdam, Netherlands; 2007. http://www.microvisionmedical.com/images/microscan2.pdf, visited 02.01.2009.
5. Dobbe J, Streekstra G, Atasever B. Measurement of functional microcircularity geometry and velocity distributions using automated image analysis. Medical and Biological Engineering and Computing. 2008;46:659–670.
6. Keimling R, Lang S. Bildfolgenanalyse in der Transplantationsmedizin am Beispiel der Leberperfusion mit orthogonaler Polarisationsspektroskopie. Lehrstuhl Intelligente Systeme, Universität Duisburg-Essen. Duisburg; 2008. Diploma Theses, http://www.uni-due.de/is, visited 02.01.2009.